Mercury stable isotope composition of seawater suggests important net gaseous elemental mercury uptake

Martin Jiskra[1,2,*], Lars-Eric Heimbürger-Boavida[2,3*], Marie-Maëlle Desgranges[3], Mariia V. Petrova[3], Aurélie Dufour[3], Beatriz Ferreira-Araujo[2], Jeremy Masbou[2], Jerome Chmeleff[2], Melilotus Thyssen[3], David Point[2], Jeroen E. Sonke[2]

[1]Environmental Geosciences, University of Basel, Switzerland

[2]Géosciences Environnement Toulouse, CNRS/IRD/Université Paul Sabatier Toulouse III, France.

[3]Aix Marseille Université, CNRS/INSU, Université de Toulon, IRD, Mediterranean Institute of Oceanography (MIO) UM 110, 13288, Marseille, France

*These authors contributed equally as 1st authors: M Jiskra, L-E Heimbürger-Boavida: martin.jiskra@unibas.ch, lars-eric.heimburger@mio.osupytheas.fr

Keywords: GEOTRACES, marine mercury, Hg stable isotopes, Mediterranean Sea, Atlantic Ocean, atmospheric deposition

Summary

Human exposure to toxic mercury (Hg) is dominated by the consumption of seafood[1,2]. Earth system models suggest that Hg in marine ecosystems is supplied by Hg(II) deposition, with a 3x smaller contribution from gaseous Hg(0) uptake, and that photochemical reduction of marine Hg(II) drives important Hg(0) evasion to the atmosphere[3,4]. Observations of marine Hg(II) deposition and gas exchange are sparse however[5], leaving the suggested importance of air-sea exchange[6] unconstrained. Here we present the first Hg stable isotope measurements of total Hg (tHg) in surface and deep Atlantic and Mediterranean seawater. We use an isotope mass balance to estimate that sea water tHg can be explained by the mixing of 41% atmospheric Hg(II) deposition and 59% Hg(0) uptake. In the particulate Hg (pHg) fraction, which includes phytoplankton at the base of the marine food web, and in a compilation of marine fish Hg isotope data, we estimate similarly important marine Hg(0) uptake fractions of 73% and 49%. We observe no photochemical odd Hg isotope anomalies in tHg, which calls into question the large model Hg(0) evasion flux. Our findings indicate that direct atmospheric Hg(0) uptake is important and has implications for our understanding of atmospheric Hg dispersal and marine ecosystem recovery.

Main text

The consumption of seafood exposes humans to mono-methylmercury (MMHg), a toxin known to affect fetal and infant neurodevelopment and cardiovascular disease in adults [1,2,7]. MMHg is formed from inorganic mercury (Hg) in the ocean and biomagnifies along marine food webs to high levels[8–10]. Anthropogenic release of Hg to the atmosphere, land and water bodies outweighs natural release at least five-fold[11,12], and is thought to have more than tripled the mercury content of surface ocean waters[13]. Climate change and overfishing also affect fish MMHg levels, and require detailed models of Hg cycling to assess future human exposure to Hg[14]. Earth system models of Hg biogeochemical cycling suggest that atmospheric Hg deposition to the open ocean is dominated by Hg(II) wet deposition (4600 Mg y^{-1}) compared to dissolution of gaseous Hg(0) (1700 Mg y^{-1}) in a 3:1 ratio[3,4]. Rivers deliver similar amounts of Hg to the oceans as atmospheric deposition (5500 Mg y^{-1}), while only 6% of river Hg is estimated to reach the open ocean[15]. Models also estimate that, of total deposited Hg, 4600 Mg y^{-1} is re-emitted to the atmosphere by (photo-)chemical and microbial photoreduction of Hg(II) to Hg(0)[3,16]. Dissolved Hg(0) concentrations in surface waters and atmospheric Hg(0) concentrations are sporadically measured simultaneously during oceanic cruises[17], and show variable Hg(0) exchange fluxes over short time periods and across different ocean basins[18]. The direction and magnitude of the large air-sea exchange of Hg(0) depends on the parametrization of the Hg(0) exchange velocity in models[19]. The absence of direct, long-term Hg(0) flux measurements over the ocean and limited

observations of Hg(II) wet and dry deposition to oceans therefore provide insufficient constraints for model validation of sea-air Hg(0) exchange, and Hg(II) deposition fluxes. This in turn hampers our capability to predict how Hg levels in the Ocean will respond to curbed anthropogenic Hg emissions under the UN Minamata Convention on Mercury, and to climate change[20–22].

In terrestrial ecosystems, Hg stable isotopes have proven to be instrumental in understanding the relative importance of Hg(II) and Hg(0) deposition[23–25]. Atmospheric Hg(0) and Hg(II) in rainfall have different mass-dependent (MDF, δ^{202}Hg) and mas-independent fractionation (MIF, Δ^{199}Hg and Δ^{200}Hg) signatures. Even-Hg MIF (Δ^{200}Hg) is thought to be generated exclusively by upper tropospheric photochemical reactions[26,27], and no Hg transformations at the Earth's surface have been shown to fractionate Δ^{200}Hg. Δ^{200}Hg is therefore considered as a conservative tracer for atmospheric Hg deposition pathways[24]. Apart from marine biota, the Hg stable isotope composition of total unfiltered Hg (tHg) has only been measured in coastal seawater of the Canadian Arctic Archipelago, suggesting that 50% to 80% of tHg originated from coastal erosion and river input[28]. Analysis of particulate Hg (pHg) isotopes at the tropical Pacific station ALOHA (22°N) suggested that atmospheric deposition of Hg(II) from rainfall was an important Hg source to the surface ocean[29]. The Hg isotopic composition of open ocean seawater, characterized by its (sub-)picomolar levels of tHg in all basins[30], including ocean-like seas such as the Mediterranean Sea[31], remains unexplored.

In this contribution we develop and apply an ultra-clean pre-concentration method for tHg isotope analysis of seawater to understand air-sea exchange of Hg. We developed the method on oligotrophic Mediterranean seawater, and complement the tHg data with samples from the North-Atlantic Ocean, and with pHg isotope measurements for both basins. We use our new tHg isotope observations together with published atmospheric Hg(II) and Hg(0) and marine pHg, sediment and fish Hg isotope data to assess the main pathways of atmospheric Hg deposition to the ocean, and discuss the plausibility of the large global marine Hg(0) evasion flux.

Results and Discussion

Sea water Hg concentrations, speciation and isotopic composition

Seawater Hg speciation and isotope composition, and procedural standard Hg isotope data are shown in Tables S3, S4. Mediterranean station K2, 20 km off-shore, is an oligotrophic reference site that was used for the 2017 GEOTRACES Hg species intercalibration cruise because the typical water masses of the open Western Mediterranean Sea are present (Figure S1). tHg concentrations at K2 in June 2017, and Feb and May 2019 (Figure 1a, Table S1, S2) are slightly surface depleted (0.8 pM), and peak at 300m depth (1.1 pM), similar to previous observations in the Western Mediterranean Sea[31,32]. Total

methylated Hg (MeHg) concentrations peak at 400-600 m, (43 % of tHg), where oxygen levels reach their minimum due to microbial remineralization of particulate organic matter[32]. Surface tHg levels in the Bay of Marseille at Endoume pier were higher, 6.0 ± 1.1 pM. In four samples from two Atlantic Ocean stations (St21, St38, Figure S1), tHg increased with depth from 0.46 to 0.83 pM and represent the mixed layer (5m, 20m), intermediate water (650m), and north-east Atlantic deep water (NEADW, 3345m)[33]. MeHg in the two Atlantic profiles were similar to Mediterranean station K2 with low levels, 0.04 pM, at the surface and elevated levels, 0.4 pM, at depth (54 % of tHg). pHg at the Mediterranean stations K1, K2 and Julio were low with a mean of 0.11 ± 0.06 pM (1σ, n=16) for the 5-800m depth range. Fram Strait pHg in Atlantic Ocean waters of the West-Spitzbergen current had higher pHg levels of 0.31 ± 0.11 pM (1σ, n=9).

tHg isotope depth profiles for δ^{202}Hg, Δ^{199}Hg and Δ^{200}Hg signatures were replicated at station K2 during two sampling cruises in February and May 2019 and show reproducible results (Figure 1). δ^{202}Hg is uniform with depth, with a median value of -0.09 ‰ (-0.31 ‰ to 0.00 ‰; median, IQR, n = 12). Overall, Δ^{199}Hg and Δ^{200}Hg are also near-zero, with median values of 0.06 and 0.01 ‰ respectively. The four North-Atlantic Ocean tHg samples show median δ^{202}Hg of -0.45 ‰, Δ^{199}Hg of 0.09‰, and Δ^{200}Hg of 0.06‰, and are therefore similar to Mediterranean waters, even at 3345m depth in NEADW. Three independent lines of evidence suggest that the tHg isotope composition of seawater is, to first order, a relatively constant feature: 1. The February and May replicate cruises to K2 station do not show any large seasonal variation in tHg isotope profiles, 2. The eight replicate samples at the Endoume pier (Table S4), covering one diurnal 24 h cycle, do not show any Hg isotope variation, and 3. The off-shore Mediterranean and Atlantic Ocean tHg isotope signatures are similar.

pHg isotopes

At station K2, pHg Δ^{199}Hg and Δ^{200}Hg were similar in June 2017 and May 2019 at all depths, while δ^{202}Hg was higher in June 2017 by 1.5‰ at 100-400m depth. In May 2019, the only occasion when tHg and pHg isotopes were determined simultaneously at station K2, δ^{202}Hg of pHg was depleted by -1.0 ‰ (-0.8 ‰ to -1.3‰; median and IQR, n = 4) relative to tHg (Figure 1). Light isotope enriched pHg may be explained by the preferential sorption of light Hg(II) isotopes to particulate organic matter[34], or by preferential bio-uptake of light isotopes by phytoplankton that is part of the particulate pool. pHg stable isotopes sampled in 2017 at two stations, Julio and K1, closer to the coast were similar to the open sea station (K2) with no clear trends in water depth or distance from the shore (Figure S3). Marine sediments, analyzed for station Julio only (700m depth, Table S4), had similar δ^{202}Hg = -0.75 ‰ $\pm$ 0.12‰, Δ^{199}Hg = 0.04 ‰ $\pm$ 0.10‰, and Δ^{200}Hg = 0.03 ‰ $\pm$ 0.06‰ (mean $\pm$ 2σ, n=4) to mean water

column pHg (K1, K2, Julio), and were similar to sediment samples taken elsewhere in the Mediterranean Sea[35,36].

Estimating atmospheric Hg(II) and Hg(0) deposition

Δ^{200}Hg has been used successfully as a conservative tracer for atmospheric Hg(0) and Hg(II) wet deposition in terrestrial ecosystems[23,23,25]. Here we use Δ^{200}Hg to quantify the combined contribution of Hg(II) wet and dry deposition, and Hg(0) gas exchange to marine tHg and pHg. In doing so, we exclude other Hg sources such as hydrothermal or river inputs. At Mediterranean station K2, this is justified by the absence of large rivers draining into the Ligurian Sea, and reflected in the open-ocean type tHg levels around 1 pM. The Rhône River reaches the Mediterranean, 100 km west of K2, at the continental shelf of the Gulf of Lions, and is carried further westward away from K2. Similarly, there is no hydrothermal activity within 500 km from the K2 station. At the Atlantic Ocean stations St21 and St38, no influence of river[15] or hydrothermal Hg inputs was found[33].

Modern, northern hemispheric Hg(II) wet deposition is characterized by a positive Δ^{200}Hg of 0.16 ‰ (0.11 ‰ to 0.22 ‰; median, IQR, n = 106), for background sites with Hg concentrations < 25 ng L^{-1}; Table S1). A new study shows that gaseous atmospheric Hg(II) forms, that are the precursor to Hg(II) in wet deposition, have the same Δ^{200}Hg as Hg(II) wet deposition in the lower free and middle troposphere[27]. A recent modeling study evaluated the origin of global Hg(II) wet and dry deposition[37], and found that Hg(II) sourced in the upper and middle troposphere constitutes 91% of the annual global Hg(II) wet deposition flux. The global contribution of the upper and middle troposphere to Hg(II) dry deposition was 52%. We therefore suggest that the median northern hemisphere rainfall Δ^{200}Hg of 0.17 ‰ is a reasonable estimate of the Δ^{200}Hg of combined wet and dry Hg(II) deposition. Atmospheric Hg(0), the larger complementary pool, exhibits slightly depleted Δ^{200}Hg of -0.05 ‰ (-0.08 ‰ to -0.02 ‰; median, IQR, n = 126, for background samples with Hg(0) concentrations < 2 ng m^{-3}; Table S1).

All seawater tHg and pHg samples, including published Pacific Ocean pHg[29], show Δ^{200}Hg values between those of atmospheric Hg(0) and Hg(II) (Figure 2 & Figure 4A). Based on a Δ^{200}Hg mixing model (Methods, Eq. 4) we estimate the fraction of Hg(II) wet and dry deposition, $f_{Hg(II)}$, to be 41% (32% to 65%, global median, IQR, n=17) in marine tHg and 27% (13 to 51%, n=61) in pHg. This implies that the majority, i.e. 59 to 73%, of marine tHg and pHg is derived from direct Hg(0) gas exchange. Current best model estimates of global Hg(II) deposition and net Hg(0) uptake to the ocean surface are 4600 Mg y^{-1} and 1700 Mg y^{-1} respectively[3]. Our marine tHg and pHg isotope observations suggest that the Hg(II) to Hg(0) net deposition balance is in fact opposite, favoring Hg(0) at the mid-latitude marine stations

we investigated. Whereas Δ^{200}Hg informs on the relative proportions of net Hg(II) and Hg(0) deposition, it cannot independently inform on Hg fluxes in mass per time units. Additional information is therefore needed to assess which number, 4600 or 1700 Mg y^{-1}, or both are incorrect. Direct Hg(II) wet and dry deposition measurements over the ocean are limited. Median Hg(II) wet deposition observed at six coastal monitoring sites between 2011 and 2015 is 1.6 µg m^{-2} y^{-1} [5], suggesting an approximate global Hg(II) wet deposition of 560 Mg y^{-1} to oceans. Model Hg(II) wet deposition generally is on the order of 60% of total Hg(II) deposition, the remaining 40% being Hg(II) dry deposition[3]. This suggests that total Hg(II) deposition to oceans may be closer to 1000 Mg y^{-1} rather than 4600 Mg y^{-1}. Applying our calculated Hg(II)/Hg(0) net deposition ratio of 41%/59%, we suggest that net Hg(0) deposition to Oceans is then on the order of 1350 Mg y^{-1}. Our combined marine and atmospheric Hg isotope mass balance lacks observations in the southern hemisphere. While this adds uncertainty to the global estimates, we suggest that the global model 3:1 Hg(II) to Hg(0) deposition ratio over oceans is in reality closer to 1:1.

We apply the same Δ^{200}Hg mass balance to published Hg isotope data in northern hemisphere marine sediments and fish (Table S2). Similar to sea water tHg and pHg, with median $f_{Hg(II)}$ of 41% and 27%, global sediments and marine fish Δ^{200}Hg suggest lower than expected $f_{Hg(II)}$ of 32% and 51% respectively. The marine sediment and fish Δ^{200}Hg data cover a much larger geographical range than our new tHg and pHg data, including South Pacific sediments, and therefore reinforce the idea that Ocean Hg(0) uptake is a globally important driver of marine ecosystem Hg levels.

Photochemical reduction of Hg(II) to Hg(0)

During photoreduction of Hg(II)-organic ligand complexes the magnetic isotope effect separates even from odd Hg isotopes[38]. Experimental photomicrobial Hg(II) photoreduction in simulated sea water medium has been shown to lead to negative Δ^{199}Hg in residual aquatic Hg(II)[39]. Here we evaluate whether the tHg and pHg data show evidence of odd-MIF, in addition to that inherited from atmospheric deposition sources. We first calculate the excess $\Delta^{199}Hg_{exc}$ in all seawater samples, defined as the difference between the measured Δ^{199}Hg in a marine sample and the expected Δ^{199}Hg, based on atmospheric inputs. The expected Δ^{199}Hg was calculated by binary mixing of Δ^{199}Hg in atmospheric Hg(II) and Hg(0) using the source contributions ($f_{Hg(II)}$) derived from Δ^{200}Hg (Methods, equations 3-4). Overall, the Δ^{199}Hg pattern in tHg and pHg of seawater and marine sediments is similar to Δ^{200}Hg and observed Δ^{199}Hg can largely be explained by a conservative mixing of atmospheric Hg(0) and Hg(II) deposition (Figure 2B). Atlantic and Mediterranean $\Delta^{199}Hg_{exc}$ was 0.03‰ (0.02 to 0.13‰; median, IQR, n = 17) in tHg and 0.01‰ (-0.07‰ to 0.08‰; median, IQR, n = 61) in pHg, which is not significant. Very low $\Delta^{199}Hg_{exc}$ were also found in marine sediments of the Mediterranean Sea (0.09‰, 0.03‰ to

0.12‰) and the Atlantic Ocean (0.06‰, 0.02 to 0.10‰). Elevated median $\Delta^{199}Hg_{exc}$ of 1.64‰ in marine fish (Table S2) can therefore be predominantly ascribed to photochemical breakdown of MMHg[40]. The absent diurnal tHg $\Delta^{199}Hg$ variation in coastal Mediterranean water, under fully sunlit (175 W m^{-2}) and high wind (10 m s^{-1}) conditions favorable of Hg(0) evasion, support slow marine Hg photoreduction. Given that odd-MIF is one of the hallmarks of aqueous Hg(II) photoreduction, the low to absent $\Delta^{199}Hg_{exc}$, <0.09‰, in marine tHg, pHg and sediment Hg suggests that the large photoreductive marine Hg(0) evasion flux of 4600 Mg y^{-1} in models is likely overestimated. This notion is also supported by the absence of seasonal Hg(0) variation in the atmospheric marine boundary layer, in particular in the ocean dominated southern hemisphere[41]. Figure 4 illustrates (in red) changes in atmosphere-ocean Hg exchange based on our findings. In order to maintain steady-state in atmospheric Hg inputs and outputs, we adjust marine Hg emissions to 600 Mg y^{-1}, which is 8x lower than the previous estimate and compatible with the low $\Delta^{199}Hg_{exc}$ observed. Lower atmospheric Hg(II) deposition to and lower Hg(0) evasion from oceans has profound impacts on the parameterization of Earth system Hg models, the lifetime of anthropogenic Hg in atmosphere and surface ocean, and consequently the anticipated recovery of ecosystems following aggressive Hg emission policy.

Acknowledgements

This work was supported by research grants ANR-17-CE34-0010 MERTOX to DP, FP7-IDEAS-ERC grant No 258537 and H2020 ERA-PLANET grant No 689443 via the iCUPE and iGOSP project, ERC-2010-429 StG_20091028, Chantier Arctique Français funding via the Pollution in the Arctic System Project to JES and LEHB, H2020 Marie Sklodowska-Curie grant No 657195 and Swiss National Science Foundation grant PZ00P2_174101 to MJ, APOG DECOMAR, MISTRALS AT P&C and the AXA RF grants to LEHB. We thank Laure Laffont for laboratory management, Olivier Grosso and Deny Malengros for technical assistance. We are grateful to Geraldine Sarthou, Pascale L'Herminer, and Helene Planquette for coordinating the 2014 GEOVIDE cruise. We thank Luisa Metral from MARBEC and Frederic Menard from MIO for providing tuna fish samples from the Mediterranean Sea. We thank Michiel Rutgers van der Loeff, Torsten Kanzow and the Alfred-Wegener-Institute for Polar and Marine Research for organizing the 2016 GRIFF cruise. We thank the captains, crew and sampling teams onboard the RV Antedon II, RV Pourquoi Pas? and FS Polarstern for their support at sea. Thanks also go to the shipboard participants, captain and crew of the N/O l'Atalante for obtaining sediment samples from the 2015 VESPA cruise. VESPA was funded by the French Ministry of Research and Higher Education, with support from the governments of New Zealand and New Caledonia.

Author contributions

LEHB, JES, MJ and DP conceived the study. LEHB, MJ, DP, MP, MVP, MMD and JES performed sampling. JES, MJ, and LEHB developed and applied the tHg isotope pre-concentration methods. JES, MJ, JM and JC performed isotope measurements. MMD, MVP, AD, LEHB, MJ, JM, DP, and MT performed additional laboratory work. MJ, JES and LEHB analyzed the data. JES and MJ wrote the draft paper, which was improved by contributions from LEHB and DP, and commented by all authors.

Methods

The method for tHg in sea water consists of an ultra-clean shipboard sampling and post-cruise sample processing protocol using a standard stannous chloride ($SnCl_2$) reduction purge-and-trap method, based on the USEPA method 1631[42].

Sampling. Repeated, daily cruises were undertaken on the RV Antedon II from Marseille (France) to the nearby (20 km) oligotrophic, off-shore station K2 (42.98 N/5.41 E/ >1500 m-depth) between 14/6/2017 and 21/6/2017, on 27/02/2019 and 22/05/2019. We used an epoxy-painted trace metal clean carousel, equipped with a conductivity-temperature-depth unit (CTD, Seabird SBE 911plus), and oxygen sensor (Seabird SBE 43), and 8x 10 L GOFLO trace metal clean bottles (General Oceanics). Samples were taken at up to 12 depths for Hg species, and at 4 depths for tHg and pHg isotopes, corresponding to surface waters (5 m), the chlorophyll-maximum (20 m), the oxygen minimum zone (400 m) and deep (800 m) waters. See SI for salinity, temperature, oxygen and fluorescence data. Unfiltered seawater was drawn *via* acid-cleaned 6 mm FEP tubing into pre-cleaned 20 L Pyrex glass bottles with GL45 PFA Teflon caps. Bottles were filled to the 20 L mark, and not to the brim, in order to preserve a 3 L headspace for purge and trap purposes. Bottles were protected from sunlight and breaking risk in 70 L plastic barrels (Kruizinga.nl Ref#53-WHV70) by using polyurethane expansive foam to fit them in the barrels. We anticipate that future use of 20 L polycarbonate carboys are an alternative option, for safer sampling during rough seas. Unfiltered seawater was drawn from each GOFLO bottle into acid-cleaned and blank-tested 60 mL FEP Teflon bottles (Nalgene) for tHg and 250 mL PFA Teflon bottles (Savillex Purillex) for MeHg, MMHg and dissolved gaseous Hg (DGM = Hg^0 + dimethyl-Hg (DMHg)) analysis. All sampling was compliant with strict GEOTRACES trace metal clean sampling procedures[43]. Eight 20 L replicate samples of seawater from the Bay of Marseille were taken every three hours on 12/11/2019 at the Endoume pier. Seawater is continuously pumped at 20 L min^{-1} into the Mediterranean Institute of Oceanography (MIO) seawater sensing lab (SSL@MM). Samples were transported to MIO and processed within 24 h. Atlantic Ocean tHg samples were collected during the GEOVIDE cruise (GEOTRACES-GA01 transect), on board the RV "Pourquoi Pas?" between 15/05/2014 and 30/06/2014. tHg values for GEOVIDE have been published elsewhere [33].

Particulate Hg. pHg was sampled using in situ pumps (McLane LV08) at stations K1 (43.10 N, 5.49 E, 700 m depth, 10 km off-shore, continental slope), K2, and Julio (43.13 N, 05.36 E, 100 m-depth, 10 km off-shore, shelf) in the Mediterranean Sea on 16/06/2017, and at K2 on 22/05/2019; in Fram Strait Atlantic waters from 21/7/2016 to 1/9/2016 during the FS Polarstern PS100 GRIFF cruise (Geotraces-GN05 transect). Pre-burnt Millipore 142mm QMA, or GF/F were deployed for 1 - 3 h to collect particles from 148-792 L of seawater. Filter samples were frozen onboard, shipped frozen to MIO, freeze dried (Christ Gamma 1-16 LSCplus), and stored in the dark until analysis. Table S4 summarizes all sampling locations.

Pre-concentration of tHg from seawater for stable isotope analysis

The 20L Mediterranean tHg samples were acidified and oxidized, within 12 h after sampling, at the MIO laboratory, using 5 mL 0.2 N BrCl (Sigma-Aldrich KBr and $KBrO_3$ salts) in concentrated bi-distilled 9 N HCl, leading to an initial sample HCl concentration of 0.0023 N. BrCl blanks were analyzed before addition, as it potentially constitutes the largest single component of the method blank. The volume of BrCl was optimized by visual inspection of the sample turning slightly yellow, indicating excess BrCl over reduced seawater components such as dissolved and particulate organic matter (DOC, POC, OM). We anticipate that the volume of BrCl added, and the time needed to convert all Hg species to labile Hg(II) forms will depend on the OM levels of seawater elsewhere. Samples were let sit for 12 h, after which a 60 mL subsample was taken with an acid cleaned, 60 cm long, burette into pre-combusted 60 mL glass vials with acid-washed Teflon-lined caps for tHg concentration analysis. This tHg subsample is compared to the shipboard 60mL tHg FEP sample and serves to verify that the 20L bottles are neither contaminated, nor subjected to tHg loss.

tHg pre-concentration was started by replacing the GL45 PFA Teflon caps (Savillex) by GL45 two-port PFA Teflon caps (Savillex) to guide 60 cm long 6 mm OD (3 - 4 mm ID) Pyrex bubbling post with a 1 cm long P3 porosity frit (VitraPOR Micro Filter-Candle, Robuglas, Germany, custom assembled by Verres Vagner, Toulouse, France). The second port on the GL45 cap hosted a 10 cm long 6 mm OD FEP tube that was connected with a short piece of 10 mm OD, 4 mm ID silicone tubing to a shorter, 25 cm long, elbowed 6mm OD Pyrex bubbling post, with 1 cm long P2 frit (VitraPOR). The P2 bubbler post was then inserted into a 60 mL, 20 cm long glass test tube, filled with 6 mL of oxidizing 40 vol% inverse aqua regia (iAR) solution. The finer P3 bubbler frit inside the bottle leads to abundant small bubbles, but can technically be replaced by coarser frits. The medium P2 bubbler frit inside the 40% iAR trap is critical to avoid over pressure and leaks of Hg(0) from the 20 L bottle. All glassware was pre-combusted at 530°C and Teflon-ware was cleaned by multiple bi-distilled HCl steps in a class 100 clean room.

Standard protocols for Hg(II) analysis by $SnCl_2$ reduction, such as EPA method 1631, use a large excess of $SnCl_2$ over Hg(II). While $SnCl_2$ does not pose a blank issue (purging it removes all Hg traces), it generates large volumes of toxic waste in each 20 L bottle after pre-concentration. We therefore tested up to 100x lower levels of anhydrous $Sn(II)Cl_2$ (Sigma-Aldrich). Hg(II) reduction by Sn(II) competes however with excess BrCl and natural oxygen present in seawater, i.e. Sn(II) is oxidized by BrCl and O_2 before it can reduce Hg(II). We therefore neutralized excess BrCl by adding 4 mL of NH_4.HCl (4.3 M) and verified disappearance of the yellow color. We then pre-purged (before adding $SnCl_2$) the 20 L sample with Hg-free argon at 300 mL min^{-1} for 3 h to remove > 90 % of dissolved oxygen. The 40% iAR solution trap was connected during pre-purging to trap any potential, though unlikely, loss of gaseous Hg from the sample. Adding $SnCl_2$ at this point, had however shown abundant precipitation of a fine white solid, presumably $SnCl_{2,s}$, which we remedied by adding an additional 80 mL volume of HCl to stabilize Sn(II) in the samples. Sn(II) addition was performed in two ways: i) 125 mL of $SnCl_2$ was slowly pumped with a peristaltic pump (Gilson) at 1.25 mL min^{-1}, and 1/16'' PFA tubing, via the central bubbling post into the bottle over 2 h; ii) the 125 mL was added instantly *via* the GL45 cap. No differences in Hg recovery were found between the two. Upon addition of $SnCl_2$ by pump or in batch, we purged the 20 L samples for 8 h at 300 mL min^{-1}, in order to quantitatively collect sample Hg into the oxidizing 40% iAR solution trap. At the end of 6 h of pre-concentration, the argon flow was stopped, and the 40 v% iAR traps removed and diluted with MQ water to 20 v% iAR and stored cold (4°C) in the dark until analysis.

For the Atlantic Ocean tHg samples, a different pre-concentration technique was applied onboard which is described in detail in the Supporting Information. In brief, 48L samples, stored in tedlar (Teflon) bags, were pumped at 5mL min^{-1}, through an iodated activated carbon (IAC) cartridge onboard. The IAC sorbent was combusted back on land, at Geosciences Environnement Toulouse (GET), in a dual tube furnace set-up, and sample Hg(0) trapped in 6 mL 40% iAR. We abandoned this method due to higher blanks, challenging Hg recoveries from IAC, and slowness of sea water sample loading (1 week).

Procedural blanks and standards

Procedural Hg blanks, representing all laboratory manipulations, cleaning procedures, reagent additions, and different operators, were determined as follows. Following pre-concentration of a batch of 8 samples for tHg, the residual Hg-free seawater solution, was conserved in the 20 L bottle, and all reagents were newly added to 8 bottles as described above. The solutions were then purged, similar to samples, for 8 hours into newly prepared 6 mL 40% iAR traps. Eight procedural standards were pre-concentrated in a similar fashion: following blanks, once more all reagents were added to the

remaining 20 L of Hg-free seawater solution, and 4 to 8 ng of NIST SRM 3133 Hg was added as internal standard to each bottle.

Particulate Hg concentration analysis

Total particulate Hg (pHg) concentrations were measured on 25 mm stamp-outs, by combustion – cold vapor atomic absorption spectrometry (CV-AAS, Leco AMA254) equipped with a low level optical cell at MIO. Certified reference material NRC MESS-3 marine sediment (93 ± 9 ng g^{-1}, 1σ) was used for quality control, with good results in the low, <1 ng Hg, range (88 ± 1 ng g^{-1}, 1σ). Remaining filter material was combusted whole on the dual tube furnace set-up at GET, following published protocols (Sun et al., 2013). In brief, filters are rolled up, inserted in a 20 mm diameter, 15 cm long quartz tube, which is plugged from both sides with quartz wool. The sample tube is then inserted in a 140 cm long quartz tube, housed in two tube furnaces. The first furnace, hosting the sample tube, was heated from room temperature to 900 °C over 6 h in an 80 mL min^{-1} flow of high purity oxygen. The released Hg(0) vapor and other volatile compounds passed through the 2nd pyrolizing oven, maintained at 1000°C continuously, and purged into a 40 vol% iAR oxidizing solution trap, that uses an elbowed, fritted, P2 porosity, Pyrex post. GF/F and GF/D filters melt at temperatures >530°C, but remain within the quartz sample tubes, blocked by the quartz wool. Final trapping solutions were diluted to 20%v iAR and stored cold in the dark until Hg concentration analysis by CV-AFS and Hg isotope analysis by MC-ICPMS. Reference material NIST SRM1632d coal was used for weekly quality control. Combustion purge and trapping recovery on samples, assessed by CV-AFS, was 104 ± 28%, 100 ± 28%, and 105 ± 21% (1σ) for the Mediterranean Sea, PS94 and PS100 cruise samples respectively.

tHg and Hg species concentration analysis

We added 40 µL of 0.2N BrCl to the 60 FEP Teflon bottles for ambient tHg analysis. Ambient tHg concentrations in 60 mL FEP Teflon bottle aliquots, in 20 L bottle aliquots before and after pre-concentration, and in 20% iAR solution traps were all analyzed in duplicate using a custom-made purge and trap system coupled to a cold vapor atomic fluorescence spectrometry (CV-AFS, Brooks Rand Model III), either at MIO, at GET, or shipboard[44]. The purge and trap system consists of 100 mL Teflon batch reactor (VWR), two electromagnetic valves (NResearch), a single gold trap (LECO), all connected by 1/8 inch FEP tubing to the CV-AFS. Seawater aliquots were 35 mL, and 20% iAR aliquots 100 uL. The CV-AFS was calibrated in the 1 - 20 pg range using NIST SRM 3133, and the NRC ORMS-5 certified reference material was always found within 10 % of the certified value (26 ± 1.3 ng L^{-1}, 1σ). MeHg, MMHg, and DGM were analyzed following our published protocols[44]. DMHg was calculated as the difference of tMeHg and MMHg, and dissolved Hg(0) as the difference of DGM and DMHg. Details are given in the SI.

Hg isotope analysis

Hg stable isotope ratios of final 20 % iAR trap solutions were measured in duplicate during two sessions by cold vapor multi-collector inductively coupled plasma mass spectrometry (CV MC-ICPMS) at the Observatoire Midi-Pyrénées, Toulouse[45,46]. We used a CETAC ASX-520 autosampler and HGX-200 CV system coupled to a Thermo-Scientific Neptune PLUS, equipped with a 10^{12} Ω resistor, attributed to the ^{198}Hg isotope in order to improve isotope ratio precision in the 20-50 mV range. Samples and standard signals at 0.25 ng g^{-1} tHg levels were generally 180 mV on the ^{202}Hg isotope, at a sample introduction flow rate of 0.75 mL min^{-1}. Thallium was not used as an internal standard, and the 203 and 205 masses were monitored to survey Hg-hydride interferences (i.e. $^{202}Hg^{1}H$, and $^{202}Hg^{1}H^{1}H$), which were found to be negligible when using standard H-cones. ^{196}Hg and ^{204}Hg were not analyzed due to low abundance, and cup configuration limitations. MDF of Hg stable isotopes is reported in small delta notation (δ) in per mil (‰) deviation from to the reference NIST 3133 Hg standard:

$$\delta^{xxx}Hg = (^{xxx/198}Hg_{sample}/\ ^{xxx/198}Hg_{NIST3133} - 1) \times 10^{3} \quad (1)$$

where 'xxx' refers to measured isotope masses: 199, 200, 201, and 202. Mass independent fractionation (MIF) is reported in capital delta notation[47], which is defined as the difference between the measured δ^{199}Hg, δ^{200}Hg, and δ^{201}Hg values and those predicted for MDF relative to δ^{202}Hg using the kinetic MDF law:

$$\Delta^{xxx}Hg = \delta^{xxx}Hg - SF^{xxx} \times \delta^{202}Hg \quad (2)$$

where SF^{xxx} is the mass-dependent scaling factor of 0.2520 for ^{199}Hg, 0.5024 for ^{200}Hg, and 0.7520 for ^{201}Hg[47].

The long-term instrumental precision was assessed through repeated analysis of the UM-Almaden and ETH-Fluka Hg standard at 0.25 ng g^{-1} during the two analysis sessions (SI Table S4). ETH-Fluka yielded values of −1.45 ± 0.20 ‰, 0.07 ± 0.11 ‰, 0.01 ± 0.14 ‰, 0.02 ± 0.09 ‰, 0.00 ± 0.18 ‰ (2σ, n = 10) for δ^{202}Hg, Δ^{199}Hg, Δ^{200}Hg, and Δ^{201}Hg respectively, in agreement with published values[48]. UM-Almaden standard yielded -0.55 ± 0.16‰, -0.03 ± 0.11‰, -0.01 ± 0.03 ‰, -0.05 ± 0.23 ‰ (2σ, n = 10) respectively, in agreement with previously reported values[38].

pHg and tHg isotope method uncertainty

Mean pre-concentration recoveries for tHg isotope analysis were 90 ± 10% (1σ, n=12) at Mediterranean station K2, 93 ± 18% (n=8) at Endoume coastal station, and 88 ± 31% (n=4) for Atlantic Ocean samples. Procedural blanks were 0.23 ± 0.08 ng Hg (1σ, n=4) for the $SnCl_2$ pre-concentration method, which is <10% of tHg in 20L of seawater, e.g. typically 3 - 4 ng of tHg in this study. $SnCl_2$ method

replication of eight 20L coastal Mediterranean samples (6 pM, analyzed at 1.6 ng g^{-1} by MC-ICPMS) shows good results with δ^{202}Hg, Δ^{199}Hg and Δ^{200}Hg 2σ uncertainties of 0.23, 0.16, and 0.06 ‰. NIST SRM 3133 procedural standards returned δ^{202}Hg, Δ^{199}Hg, Δ^{200}Hg, and Δ^{201}Hg values of 0.07 ± 0.23 ‰, -0.05 ± 0.16 ‰, 0.00 ± 0.06 ‰, -0.01 ± 0.18 ‰, 0.02 ± 0.21 ‰ and a mean recovery of 86 ± 16% (2σ, n = 8), suggesting no bias in the method.

pHg quality control results on NIST SRM 1632d yielded values of −1.75 ± 0.24 ‰, -0.04 ± 0.04 ‰, 0.00 ± 0.04 ‰, -0.02 ± 0.08 ‰ (2σ, n = 10) for δ^{202}Hg, Δ^{199}Hg, Δ^{200}Hg and Δ^{201}Hg respectively, in agreement with published values [45,49]. The 2σ uncertainty on pHg samples was taken to be the larger of either replicate sample analysis, procedural standard NIST SRM1632d, or secondary reference materials UM-Almaden or ETH-Fluka.

Most seawater pHg and tHg samples were analyzed in duplicate on different days. The final 2σ uncertainties reported for Mediterranean Sea and Atlantic Ocean pHg and tHg samples are the larger of the duplicate sample analysis, the 2σ on the eight NIST procedural standards (tHg), the 2σ on the ten NIST SRM 1632d standards, or the 2σ of the ETH Fluka or UM-ALmaden standards.

Stable isotope data analysis

The fraction of Hg in marine samples derived from atmospheric Hg(II) wet and dry deposition ($f_{Hg(II)}$) was calculated using a conservative mixing model as follows:

$$\Delta^{200}Hg_{sample} = f_{Hg(II)} \times \Delta^{200}Hg_{Hg(II)} + (1- f_{Hg(II)}) \times \Delta^{200}Hg_{Hg(0)} \quad (3)$$

where $\Delta^{200}Hg_{sample}$ represents the median observed value of different marine Hg pools (THg, pHg, sediment THg, fish THg), $\Delta^{200}Hg_{Hg(II)}$ and $\Delta^{200}Hg_{Hg(0)}$ the median values of previously published northern hemisphere samples for gaseous and rainfall Hg(II), and atmospheric Hg(0), respectively. The excess Δ^{199}Hg in the different marine Hg pools ($\Delta^{199}Hg_{exc}$), representing the Δ^{199}Hg which was produced within the marine system, was calculated as follows:

$$\Delta^{199}Hg_{exc} = \Delta^{199}Hg_{exc} - (f_{Hg(II)} \times \Delta^{199}Hg_{Hg(II)} + (1- f_{Hg(II)}) \times \Delta^{199}Hg_{Hg(0)}) \quad (4)$$

where $f_{Hg(II)}$ was derived from the Δ^{200}Hg of the sample according to eq. 3.

Figures

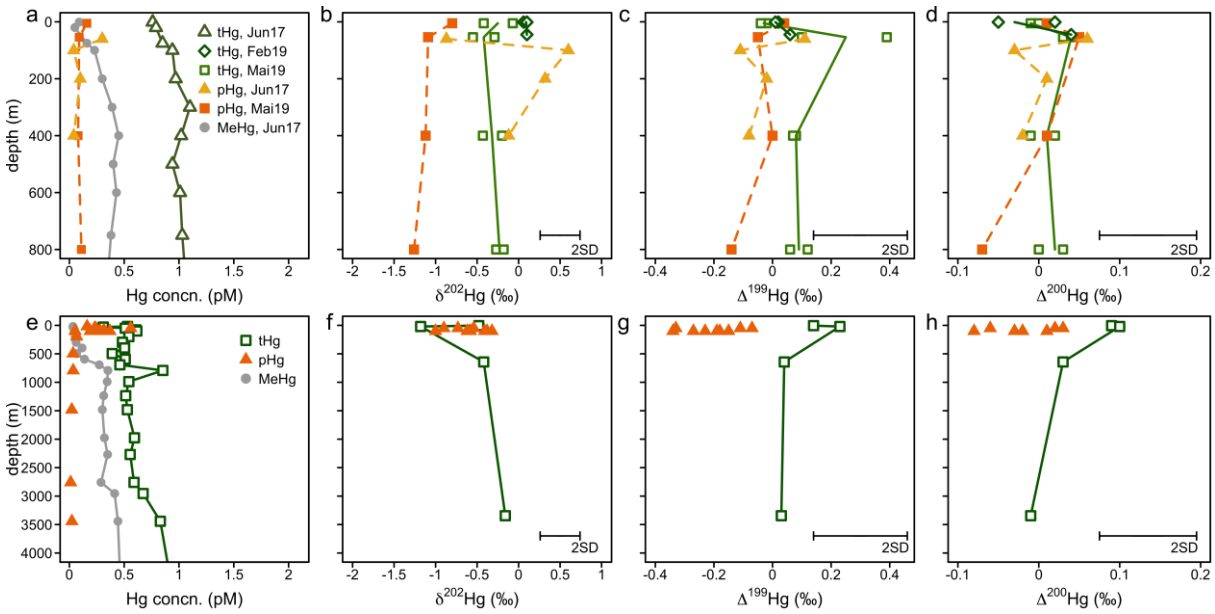

Figure 1a-h. Depth profiles of seawater Hg species concentrations and total and particulate Hg stable isotope composition at station K2 in the Mediterranean Sea (a-d) and the North Atlantic (e-h). a and e: tHg, pHg, and MeHg concentrations in pmol L^{-1} (pM). **b and f**: mass-dependent fractionation ($\delta^{202}Hg$), **c and g**: odd mass-independent fractionation ($\Delta^{199}Hg$), **d and h**: even mass-independent fractionation ($\Delta^{200}Hg$). Open symbols represent values for tHg and filled symbols pHg. The lines represent averages of replicate analysis of the same sample. Two standard deviation (2SD) uncertainties on Hg concentrations are 10%.

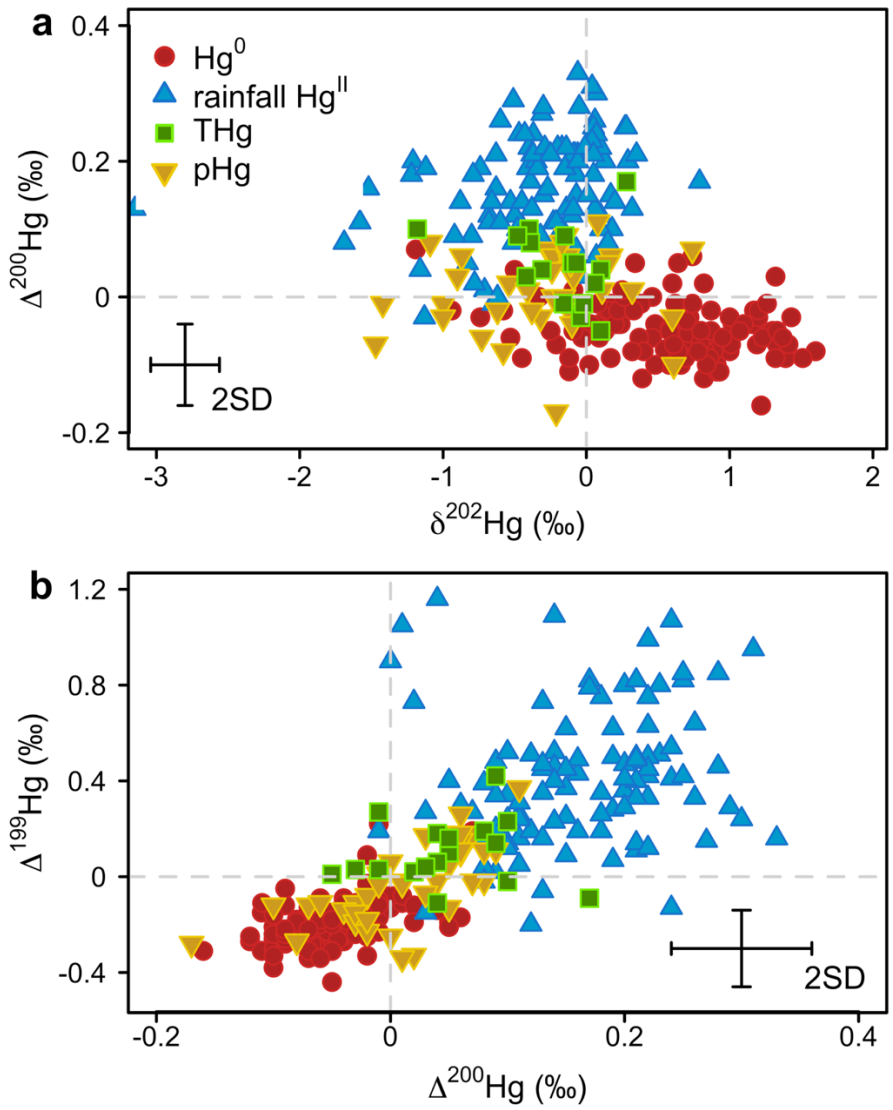

410

411 **Figure 2. Hg stable isotope composition of atmospheric sources (gaseous Hg(0) and Hg(II) in rainfall)**
412 **and seawater (total (HgT) and particulate (pHg)).** a) even mass independent fractionation (Δ^{200}Hg) vs.
413 mass dependent fractionation (δ^{202}Hg), and b) odd mass independent fractionation (Δ^{200}Hg) vs. even
414 mass independent fractionation (Δ^{200}Hg). Values of atmospheric sources are from literature (see Table
415 S1), tHg values are from this study, pHg from this study and ref.[29]. Error bars represent the 2SD of
416 replicate procedural standards for tHg and pHg.

417

418

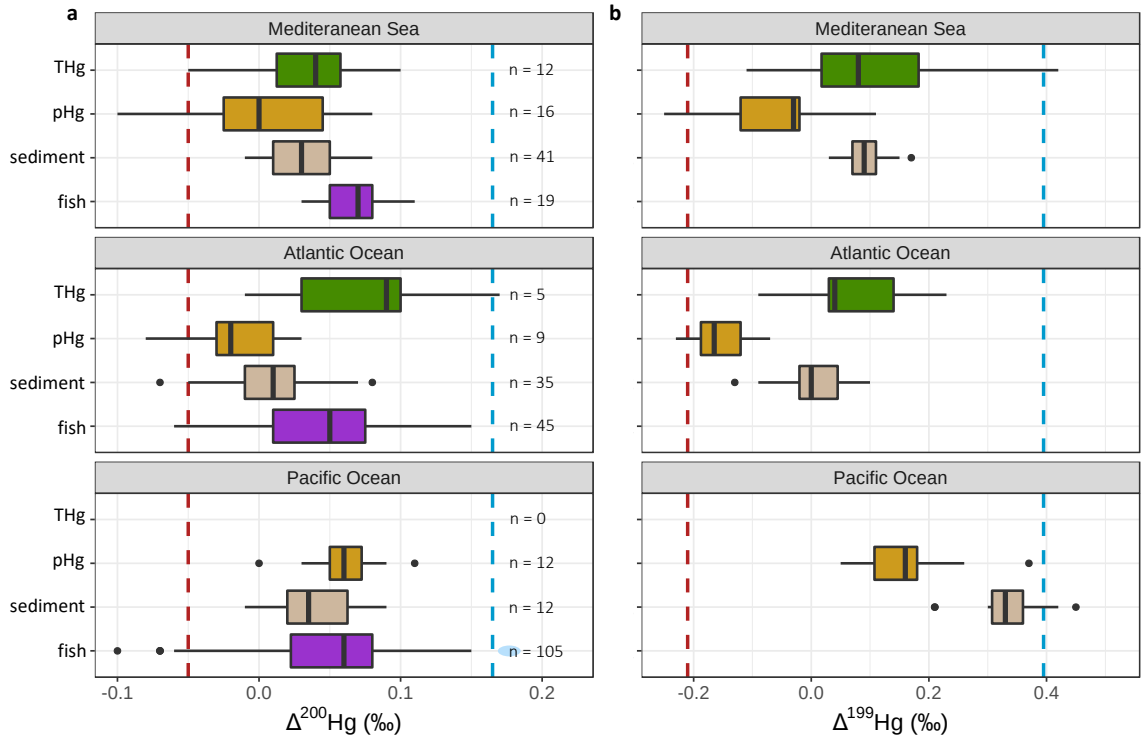

419

420 **Figure 3. Hg stable isotope signatures in different ocean basins of total Hg (tHg) and particulate Hg**
421 **(pHg) in seawater, marine sediments and marine fish. a: Even mass-independent signature (Δ^{200}Hg)**
422 **and b: Odd mass-independent signature (Δ^{199}Hg).** tHg values are from this study, pHg from this study
423 and from Motta et al. (2019), data for sediments and biota are from literature. The atmospheric
424 sources are shown in red for Hg(0) and blue for Hg(II) in rainfall, the dashed line represents the median
425 and the shaded area the interquartile range. For fish, Δ^{199}Hg are not shown in this Figure as these
426 values are heavily affected by MMHg photo-demethylation (See SI Table S2).

427

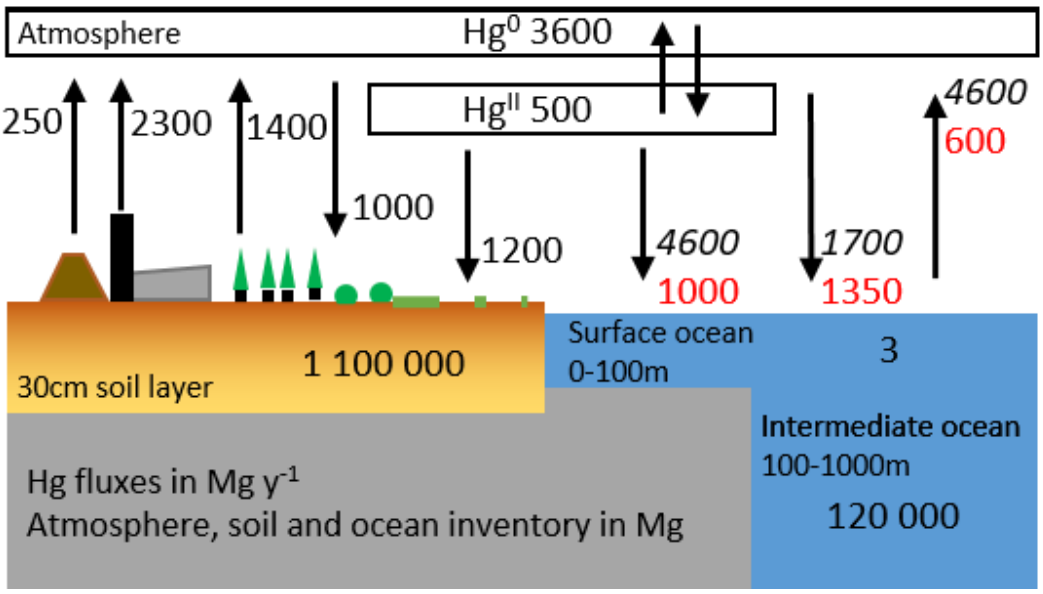

428

429 **Figure 4. Global budget of air-sea and air-land exchange.** New Hg isotope based fluxes (Mg y^{-1}) are
430 shown in red. All other Hg fluxes and atmospheric Hg0 and HgII inventory are from ref.[50]. The upper
431 30cm soil and surface (0-100m) and intermediate (100-1000m) ocean inventories are from refs.[11,51].

432

References

1. Sheehan, M. C. *et al.* Global methylmercury exposure from seafood consumption and risk of developmental neurotoxicity: a systematic review. *Bulletin of the World Health Organization* **92**, 254–269 (2014).
2. Sunderland, E. M. Mercury Exposure from Domestic and Imported Estuarine and Marine Fish in the U.S. Seafood Market. *Environmental Health Perspectives* **115**, (2007).
3. Horowitz, H. M. *et al.* A new mechanism for atmospheric mercury redox chemistry: implications for the global mercury budget. *Atmospheric Chemistry and Physics* **17**, 6353–6371 (2017).
4. Travnikov, O. *et al.* Multi-model study of mercury dispersion in the atmosphere: atmospheric processes and model evaluation. *ATMOSPHERIC CHEMISTRY AND PHYSICS* **17**, 5271–5295 (2017).
5. Sprovieri, F. *et al.* Five-year records of mercury wet deposition flux at GMOS sites in the Northern and Southern hemispheres. *ATMOSPHERIC CHEMISTRY AND PHYSICS* **17**, 2689–2708 (2017).
6. Zhang, Y. *et al.* A Coupled Global Atmosphere-Ocean Model for Air-Sea Exchange of Mercury: Insights into Wet Deposition and Atmospheric Redox Chemistry. *Environmental Science & Technology* **53**, 5052–5061 (2019).
7. Roman, H. A. *et al.* Evaluation of the cardiovascular effects of methylmercury exposures: current evidence supports development of a dose-response function for regulatory benefits analysis. *Environ Health Perspect* **119**, 607–614 (2011).
8. Mason, R. P. & Fitzgerald, W. F. Alkylmercury species in the Equatorial Pacific. *Nature* **347**, 457–459 (1990).
9. Selin, N. E. Global Biogeochemical Cycling of Mercury: A Review. in *Annual Review of Environment and Resources* vol. 34 43–63 (2009).
10. Fitzgerald, W. F. & Lamborg, C. H. Geochemistry of Mercury in the Environment. in *Treatise on Geochemistry* (eds. Holland, E. D. & Turekian, K. K.) vol. 9 107–148 (Elsevier-Pergamon, 2004).

11. Outridge, P. M., Mason, R. P., Wang, F., Guerrero, S. & Heimbürger-Boavida, L. E. Updated Global and Oceanic Mercury Budgets for the United Nations Global Mercury Assessment 2018. *Environ. Sci. Technol.* **52**, 11466–11477 (2018).
12. Amos, H. M. *et al.* Observational and Modeling Constraints on Global Anthropogenic Enrichment of Mercury. *Environmental Science & Technology* **49**, 4036–4047 (2015).
13. Lamborg, C. H. *et al.* A global ocean inventory of anthropogenic mercury based on water column measurements. *Nature* **512**, (2014).
14. Schartup, A. T. *et al.* Climate change and overfishing increase neurotoxicant in marine predators. *Nature* **572**, 648–650 (2019).
15. Zhang, Y. *et al.* Biogeochemical drivers of the fate of riverine mercury discharged to the global and Arctic oceans. *Global Biogeochemical Cycles* **29**, 854–864 (2015).
16. Zhang, Y., Jaegle, L., Thompson, L. & Streets, D. G. Six centuries of changing oceanic mercury. *Global Biogeochemical Cycles* **28**, 1251–1261 (2014).
17. Soerensen, A. L., Skov, H., Jacob, D. J., Soerensen, B. T. & Johnson, M. S. Global Concentrations of Gaseous Elemental Mercury and Reactive Gaseous Mercury in the Marine Boundary Layer. *ENVIRONMENTAL SCIENCE & TECHNOLOGY* **44**, 7425–7430 (2010).
18. Mason, R. P. *et al.* The air-sea exchange of mercury in the low latitude Pacific and Atlantic Oceans. *Deep Sea Research Part I: Oceanographic Research Papers* **122**, 17–28 (2017).
19. Zhang, Y. *et al.* A Coupled Global Atmosphere-Ocean Model for Air-Sea Exchange of Mercury: Insights into Wet Deposition and Atmospheric Redox Chemistry. *ENVIRONMENTAL SCIENCE & TECHNOLOGY* **53**, 5052–5061 (2019).
20. Outridge, P. M., Mason, R. P., Wang, F., Guerrero, S. & Heimburger-Boavida, L. E. Updated Global and Oceanic Mercury Budgets for the United Nations Global Mercury Assessment 2018. *ENVIRONMENTAL SCIENCE & TECHNOLOGY* **52**, 11466–11477 (2018).

21. Wang, F. *et al.* How closely do mercury trends in fish and other aquatic wildlife track those in the atmosphere? - Implications for evaluating the effectiveness of the Minamata Convention. *SCIENCE OF THE TOTAL ENVIRONMENT* **674**, 58–70 (2019).
22. Krabbenhoft, D. P. & Sunderland, E. M. Global change and mercury. *Science* **341**, 1457–1458 (2013).
23. Demers, J. D., Blum, J. D. & Zak, D. R. Mercury isotopes in a forested ecosystem: Implications for air-surface exchange dynamics and the global mercury cycle. *Global Biogeochemical Cycles* **27**, 222–238 (2013).
24. Enrico, M. *et al.* Atmospheric mercury transfer to peat bogs dominated by gaseous elemental mercury dry deposition. *Environmental Science & Technology* (2016) doi:10.1021/acs.est.5b06058.
25. Obrist, D. *et al.* Tundra uptake of atmospheric elemental mercury drives Arctic mercury pollution. *Nature* **547**, 201-+ (2017).
26. Chen, J., Hintelmann, H., Feng, X. & Dimock, B. Unusual fractionation of both odd and even mercury isotopes in precipitation from Peterborough, ON, Canada. *Geochimica et Cosmochimica Acta* **90**, 33–46 (2012).
27. Fu, X. W. *et al.* Mass independent fractionation of even and odd mercury isotopes during tropospheric mercury oxidation. *EarthArXiv* (2020) doi: 10.31223/osf.io/k5dwt https://eartharxiv.org/k5dwt/.
28. Strok, M., Baya, P. A. & Hintelmann, H. The mercury isotope composition of Arctic coastal seawater. *Comptes Rendus Geoscience* **347**, 368–376 (2015).
29. Motta, L. C. *et al.* Mercury Cycling in the North Pacific Subtropical Gyre as Revealed by Mercury Stable Isotope Ratios. *Global Biogeochemical Cycles* **33**, 777–794 (2019).
30. Bowman, K. L., Lamborg, C. H. & Agather, A. M. A global perspective on mercury cycling in the ocean. *SCIENCE OF THE TOTAL ENVIRONMENT* **710**, (2020).

31. Cossa, D., Averty, B. & Pirrone, N. The origin of methylmercury in open Mediterranean waters. *Limnology and Oceanography* **54**, 3 (2009).
32. Heimbürger, L.-E. *et al.* Methyl mercury distributions in relation to the presence of nanoand picophytoplankton in an oceanic water column (Ligurian Sea, North-western Mediterranean). *Geochimica et Cosmochimica Acta* **74**, 5549–5559 (2010).
33. Cossa, D. *et al.* Mercury distribution and transport in the North Atlantic Ocean along the GEOTRACES-GA01 transect. *BIOGEOSCIENCES* **15**, 2309–2323 (2018).
34. Wiederhold, J. G. *et al.* Equilibrium mercury isotope fractionation between dissolved Hg(II) species and thiol-bound Hg. *Environmental Science and Technology* **44**, 4191–4197 (2010).
35. Gehrke, G. E., Blum, J. D. & Meyers, P. A. The geochemical behavior and isotopic composition of Hg in a mid-Pleistocene western Mediterranean sapropel. *Geochimica et Cosmochimca Acta* **73**, 1651–1665 (2009).
36. Ogrinc, N., Hintelmann, H., Kotnik, J., Horvatl, M. & Pirrone, N. Sources of mercury in deep-sea sediments of the Mediterranean Sea as revealed by mercury stable isotopes. *Scientific Reports* **9**, 11626 (2019).
37. Shah, V. & Jaegle, L. Subtropical subsidence and surface deposition of oxidized mercury produced in the free troposphere. *ATMOSPHERIC CHEMISTRY AND PHYSICS* **17**, 8999–9017 (2017).
38. Bergquist, B. A. & Blum, J. D. Mass-Dependent and -Independent Fractionation of Hg Isotopes by Photoreduction in Aquatic Systems. *Science* **318**, 417–420 (2007).
39. Kritee, K., Motta, L. C., Blum, J. D., Tsui, M. T.-K. & Reinfelder, J. R. Photomicrobial Visible Light-Induced Magnetic Mass Independent Fractionation of Mercury in a Marine Microalga. *ACS EARTH AND SPACE CHEMISTRY* **2**, 432–440 (2018).
40. Blum, J. D., Popp, B. N., Drazen, J. C., Choy, C. N. & Johnson, M. W. Methylmercury production below the mixed layer in the North Pacific Ocean. *Nature Geoscience* **DOI: 10.1038/NGEO1918**, (2013).

41. Jiskra, M. *et al.* A vegetation control on seasonal variations in global atmospheric mercury concentrations. *NATURE GEOSCIENCE* **11**, 244+ (2018).
42. USEPA. method 1631 Revision EMercury in Water by Oxidation, Purge and Trap, and Cold Vapor Atomic Fluorescence Spectrometry, EPA-821/R-02/019, Washington, D.C., United States Environmental Protection Agency, Office of Water (2002). (2002).
43. Cutter, G. J. *et al.* Sampling and Sample-handling Protocols for GEOTRACES Cruises. Version 3.0. (2017).
44. Heimbürger, L. E. *et al.* Shallow methylmercury production in the marginal sea ice zone of the central Arctic Ocean. *Scientific Reports* **doi:10.1038/srep10318**, (2015).
45. Sun, R., Enrico, M., Heimbürger, L.-E., Scott, C. & Sonke, J. E. A double-stage tube furnace-acid-trapping protocol for the pre-concentration of mercury from solid samples for isotopic analysis. *Analytical and Bioanalytical Chemistry* **405**, 6771–6781 (2013).
46. Jiskra, M., Sonke, J. E., Agnan, Y., Helmig, D. & Obrist, D. Insights from mercury stable isotopes on terrestrial-atmosphere exchange of Hg(0) in the Arctic tundra. *Biogeosciences* **16**, 4051–4064 (2019).
47. Blum, J. D. & Bergquist, B. A. Reporting of variations in the natural isotopic composition of mercury. *Analytical and Bioanalytical Chemistry* **388**, 353–359 (2007).
48. Jiskra, M. *et al.* Mercury Deposition and Re-emission Pathways in Boreal Forest Soils Investigated with Hg Isotope Signatures. *Environmental Science & Technology* **49**, 7188–7196 (2015).
49. Zheng, L. *et al.* Mercury stable isotope compositions in magmatic-affected coal deposits: New insights to mercury sources, migration and enrichment. *CHEMICAL GEOLOGY* **479**, 86–101 (2018).
50. Horowitz, H. M., Jacob, D. J., Amos, H. M., Streets, D. G. & Sunderland, E. M. Historical Mercury Releases from Commercial Products: Global Environmental Implications. *Environmental Science & Technology* **48**, 10242 (2014).

51. Lim, A. G. *et al.* A revised northern soil Hg pool, based on western Siberia permafrost peat Hg and carbon observations. *Biogeosciences* **2020**, 1–35 (2020).

Online Supporting Information to:

Mercury stable isotope composition of seawater suggests important net gaseous elemental mercury uptake

Martin Jiskra[1,2,*], Lars-Eric Heimbürger-Boavida[2,3*], Marie-Maëlle Desgranges[3], Mariia V. Petrova[3], Aurélie Dufour[3], Beatriz Ferreira-Araujo[2], Jeremy Masbou[2], Jerome Chmeleff[2], Melilotus Thyssen[3], David Point[2], Jeroen E. Sonke[2]

[1]Environmental Geosciences, University of Basel, Switzerland

[2]Géosciences Environnement Toulouse, CNRS/IRD/Université Paul Sabatier Toulouse III, France.

[3]Aix Marseille Université, CNRS/INSU, Université de Toulon, IRD, Mediterranean Institute of Oceanography (MIO) UM 110, 13288, Marseille, France

*These authors contributed equally as 1st authors: M Jiskra, L-E Heimbürger-Boavida: martin.jiskra@unibas.ch, lars-eric.heimburger@mio.osupytheas.fr

Materials and Methods

Rationale

tHg concentration in seawater is the sum of several operationally defined species, including dissolved gaseous Hg(0), dissolved gaseous dimethyl-Hg (DMHg), dissolved inorganic Hg(II) compounds, dissolved monomethyl-Hg compounds (MMHg), and particulate-bound Hg(II) and MMHg compounds (pHg). Both concentration and stable isotope analysis of tHg in seawater require the transformation of these compounds to dissolved, labile Hg(II) forms by addition of a strong oxidant such as BrCl, prepared in concentrated HCl. The concomitant oxidation and acidification also inhibits biological activity, stabilizes Hg(II) in solution and minimizes potential losses to sampling container walls or to the atmosphere. Two criteria need to be met for a robust Hg stable isotope analysis of seawater: first, the low-picomolar seawater concentration has to be concentrated to levels suitable for Hg stable isotope analysis (typically 0.2 – 1 ng mL^{-1} or 1 – 5 nM). This pre-concentration needs to be quantitative in order to avoid Hg isotope fractionation during transfer. Second, the procedural blank of the method needs to be low, ideally below 10% of the total amount of Hg in the sample. Low blank levels rely on ultra-clean sampling at sea, clean sampling vessels and ultra-low Hg levels of reagents used.

Previous studies have successfully developed methods for large volume (1 - 20 L) pre-concentration of tHg from natural waters, including rain, snow, ice, lake and coastal seawater. Gratz et al. (2010) and Sherman et al. (2010) first used continuous cold vapor generation, with $SnCl_2$ as a reductant, to pre-concentrate 1 - 4 L of snow and rainfall samples into small volume (25 mL) 2 % (w/w) oxidizing $KMnO_4/H_2SO_4$ solution trap [1,2]. This method was later modified to a batch-reactor set-up to pre-concentrate 1 L of rainfall in a 2 L Pyrex bottle, by slow, pumped addition of $SnCl_2$, and identical $KMnO_4/H_2SO_4$ solution trap [3] and trapping solutions of 40 vol% inverse *aqua regia* (iAR, 4.2 N HNO_3, 1.2 N HCl; [4]). Finally, in Obrist et al. (2017) we scaled up the batch purge and trap method to handle up to 20 L of snow and rain sample [5]. An alternative method was developed by Chen et al. (2016) using the AG-1-X4 anion exchange resin to pre-concentrate >40 ng of tHg from freshwater lakes [6]. $HgCl_4^{2-}$ in the acidified, 0.1 N HCl, sample is pumped at 3.5 mL min^{-1} over 0.5 mL of AG-1-X4 resin. Sorbed Hg is then eluted with 10 mL of 0.05 % L-cysteine in 0.5 N HNO_3, oxidized by BrCl, neutralized with NH_4OH and analyzed by MC-ICPMS. Štrok et al. (2015) optimized the anion exchange resin method for seawater and published the first Hg stable isotope data of coastal seawater (1.5-3.1 pM) from the Canadian Arctic Archipelago [7]. The latter two methods by Štrok et al. (2015) and Obrist et al. (2017) are capable of handling sample volumes of 20 L or more that are necessary for background level tHg pre-concentration from seawater (0.4 to 1.5 pM). Our objective was therefore to adapt our existing

large volume pre-concentration protocol, based on $SnCl_2$ reduction, for rain and snow to seawater. We optimized the protocol for quantitative pre-concentration yields and low blank levels.

Pre-concentration troubleshooting, Sn waste disposal and bottle cleaning

During pre-concentration the 20L sample bottle is under argon over-pressure in order to generate a fine stream of bubbles. It is therefore important at the end of pre-concentration, or during troubleshooting, not to vent the argon supply tube to the 20L sample bottle and release argon pressure. The reason is that with the 20 L bottle under over-pressure, venting the argon supply tube results in a sudden pressure drop, and acidified sample solution with $SnCl_2$ moving from the 20 L bottle into the tall bubbler post, possibly all the way to the argon flow regulator, damaging the latter. Worse, the 40 vol% iAR trap solution is aspirated up into its short bubbler post and into the 20 L bottle, resulting in the loss of the sample. Using our final optimized Sn addition protocol, each 20 L bottle contains at the end of a pre-concentration run, 2.5 g of Sn(II), and should be disposed of following local environmental regulations. If needed, the dissolved Sn(II) concentration can be lowered by hydrogen peroxide addition, which quantitatively precipitates $Sn(IV)O_2$, that can then be filtered or decanted. Quantitative oxidation of Sn(II) by hydrogen peroxide also has the advantage that no traces of Sn(II) remain in the 20 L bottle, which can be acid-cleaned and rinsed with abundant MQ water to receive the next batch of seawater samples. In this study both sampling and pre-concentration were done in the same bottle. We expect however that the use of separate bottles, possibly using plastic 20 L carboys at sea for safety, does not increase blanks.

Alternative, activated carbon based pre-concentration method for sea water

We have, over the past years, tested an alternative method for low-level Hg pre-concentration in order to measure Hg isotopes in sea water. The method uses small 200 mg iodated activated carbon powder (Brooks Rand) cartridges, over which large volumes (50L) of sea water are pumped at a slow flow rate of 5 ml min^{-1}. Following laboratory recovery and blank testing, we applied the method during the 2014 GEOTRACES Geovides cruise in the North-Atlantic Ocean. Unfiltered seawater was transferred using clean 6mm FEP tubing from GOFLO bottles into acid washed 50L tedlar bags. A peristaltic pump, with 1.14mm ID (red/red) tygon pump tubing was used to load samples on the IAC traps during 1 week. Traps were dried for 5 min in a dry high purity argon stream, sealed with silicone stoppers and stored and transported dry and in the dark to the GET laboratory. The IAC powder was combusted using a dual tube furnace combustion method [8]. IAC blanks were 0.5 ng Hg per 200mg of IAC traps, and sample recoveries were 88 ± 31%. In hindsight, it has been difficult to fully recover Hg from IAC traps due to abundant volatile iodine release and transfer to oxidizing solution traps. We recommend that further

development of activated carbon based methods use commercial sulfur impregnated activated carbon (Calgon HGR), which does not have this issue.

MMHg and DMHg analysis

MMHg and DMHg were determined by isotope dilution (ID)- gas chromatography – sector field ICP-MS (ID-GC-SF-ICPMS) method at the MIO laboratory, following previously published protocols[9]. First the sum of both species (tMeHg) was quantified on an acidified sample that converts DMHg to MMHg. A second replicate sample was purged to remove DMHg before acidification, allowing direct measurement of MMHg. DMHg was calculated by difference, as tMeHg – MMHg. In both sample aliquots MMHg and inorganic Hg species were extracted after derivatization. In brief, enriched spikes of ^{199}iHg and ^{201}MeHg (ISC Science, Spain) were added to a 115 mL aliquot of the sea water samples. After 24h of equilibration, pH was adjusted to 3.9 with NH_3 (ULTREX® II Ultrapure Reagent, J.T. Baker, USA) and a buffer solution made up with acetic acid (glacial, ULTREX® II Ultrapure Reagent, J.T. Baker, USA) / sodium acetate (J.T. Baker, USA). A solution of 1 % (v:v) sodium tetra propyl borate (Merseburger Spezialchemikalien, Germany) was made up freshly, under cold conditions and avoiding contact with atmospheric oxygen. 1 mL of this solution was then added together with 200 µL hexane (Sigma Aldrich, USA). The glass bottles were hermetically sealed with Teflon-lined caps and vigorously shaken for 15 minutes. The organic phase was recovered and injected in the GC (Thermo Trace Ultra), coupled to a sector field ICPMS (Thermo Element XR). Detection limits were 0.005 pM for MMHg, and 0.01 pM for DMHg.

Table S1: Summary of Hg stable isotope data used for Figure 2 and calculations. *sediments considered below 1000m water depth.

Pool	Ocean Basin	n	Hg concn.			δ^{202}Hg (‰)		Δ^{199}Hg (‰)		Δ^{200}Hg (‰)		Reference
			median	IQR	Units	median	IQR	median	IQR	median	IQR	
Hg(II) rainfall		106	13	(9 to 18)	ng/L	-0.30	(-0.63 to 0.03)	0.39	(0.21 to 0.52)	0.16	(0.11 to 0.22)	[1,3,4,10–14]
Hg(0)		126	1.23	(1.08 to 1.45)	ng/m^3	0.61	(0.16 to 0.90)	-0.21	(-0.24 to -0.15)	-0.05	(-0.08 to -0.02)	[2,4,5,10,15–17]
tHg	**All samples**	17				-0.15	(-0.39 to -0.02)	0.06	(0.02 to 0.18)	0.04	(0.02 to 0.09)	this study
	Med. Sea	12				-0.08	(-0.31 to 0.00)	0.08	(0.02 to 0.18)	0.04	(0.01 to 0.06)	this study
	Atlantic	5				-0.42	(-0.48 to -0.16)	0.04	(0.03 to 0.14)	0.09	(0.03 to 0.10)	this study
pHg	**All samples**	37				-0.22	(-0.58 to -0.10)	-0.03	(-0.14 to 0.11)	0.01	(-0.02 to 0.06)	this study, [11]
	Med. Sea	16				-0.14	(-0.9 to 0.19)	-0.05	(-0.12 to -0.02)	0.00	(-0.03 to 0.04)	this study
	Atlantic	9				-0.58	(-0.73 to -0.41)	-0.19	(-0.27 to -0.15)	-0.02	(-0.03 to 0.03)	this study
	Pacific	12				-0.13	(-0.22 to -0.1)	0.16	(0.1 to 0.18)	0.06	(0.05 to 0.07)	[11]
sediment	**All samples**	88	55	(34to 86)	ng/g	-0.82	(-1.21 to -0.45)	0.07	(0.02 to 0.11)	0.02	(0.01 to 0.04)	
	Med. Sea	41	53	(44 to 83)	ng/g	-1.14	(-1.61 to -0.86)	0.09	(0.07 to 0.11)	0.03	(0.01 to 0.05)	This study, [17, 18]
	Atlantic	35	55	(33 to 137)	ng/g	-0.40	(-0.60 to 0.32)	0.00	(-0.02 to 0.05)	0.01	(-0.01 to 0.03)	[18,19*]
	Pacific	12	52	(20 to 74)	ng/g	-1.58	(-2.5 to -0.5)	0.33	(0.30 to 0.36)	0.04	(0.02 to 0.06)	this study
fish	**All samples**	169	252	(81 to 1403)	ng/g	0.49	(0.28 to 0.79)	1.72	(1.35 to 1.98)	0.06	(0.03 to 0.08)	
	Med. Sea	19	2950	(2460 to 3826)	ng/g	0.37	(0.29 to 0.47)	1.78	(1.70 to 1.81)	0.07	(0.05 to 0.08)	this study
	Atlantic	45	105	(60 to 190)	ng/g	0.34	(0.26 to 0.45)	1.32	(1.06 to 1.50)	0.05	(0.01 to 0.08)	[20,21]
	Pacific	105	366	(104 to 747)	ng/g	0.71	(0.35 to 0.89)	1.84	(1.48 to 2.17)	0.06	(0.02 to 0.08)	[22–24]

Table S2: Modeled contribution of Hg(II) from wet and dry deposition, $f_{Hg(II)}$, and excess $\Delta^{199}Hg_{exc}$ according to Methods Equations 3, 4. Excess $\Delta^{199}Hg_{exc}$ represents sample $\Delta^{199}Hg$ acquired by Hg(II) photoreduction in sea water, in addition to the $\Delta^{199}Hg$ inherited from atmospheric Hg deposition.

Pool	Ocean Basin	n	$f_{Hg(II)}$		$\Delta^{199}Hg_{exc}$ (‰)	
			median	IQR	median	IQR
tHg sea water	**All samples**	17	0.41	(0.32 to 0.65)	0.03	(0.02 to 0.13)
	Med. Sea	12	0.41	(0.29 to 0.50)	0.06	(0.03 to 0.19)
	Atlantic	5	0.65	(0.37 to 0.69)	0.02	(-0.04 to 0.02)
pHg sea water	**All samples**	37	0.27	(0.13 to 0.51)	0.01	(-0.07 to 0.08)
	Med. Sea	16	0.20	(0.08 to 0.43)	0.02	(-0.08 to 0.05)
	Atlantic	9	0.13	(0.09 to 0.27)	-0.06	(-0.10 to -0.04)
	Pacific	12	0.51	(0.46 to 0.57)	0.07	(0.00 to 0.13)
marine sediment	**All samples**	88	0.32	(0.28 to 0.41)	0.09	(0.03 to 0.12)
	Med. Sea	41	0.37	(0.28 to 0.47)	0.09	(0.03 to 0.12)
	Atlantic	35	0.28	(0.18 to 0.35)	0.06	(0.02 to 0.10)
	Pacific	12	0.40	(0.32 to 0.52)	0.25	(0.23 to 0.33)
fish	**All samples**	169	0.51	(0.37 to 0.60)	1.64	(1.28 to 1.92)
	Med. Sea	19	0.55	(0.46 to 0.60)	1.65	(1.56 to 1.72)
	Atlantic	45	0.46	(0.28 to 0.58)	1.29	(1.00 to 1.40)
	Pacific	105	0.51	(0.32 to 0.60)	1.79	(1.47 to 2.08)

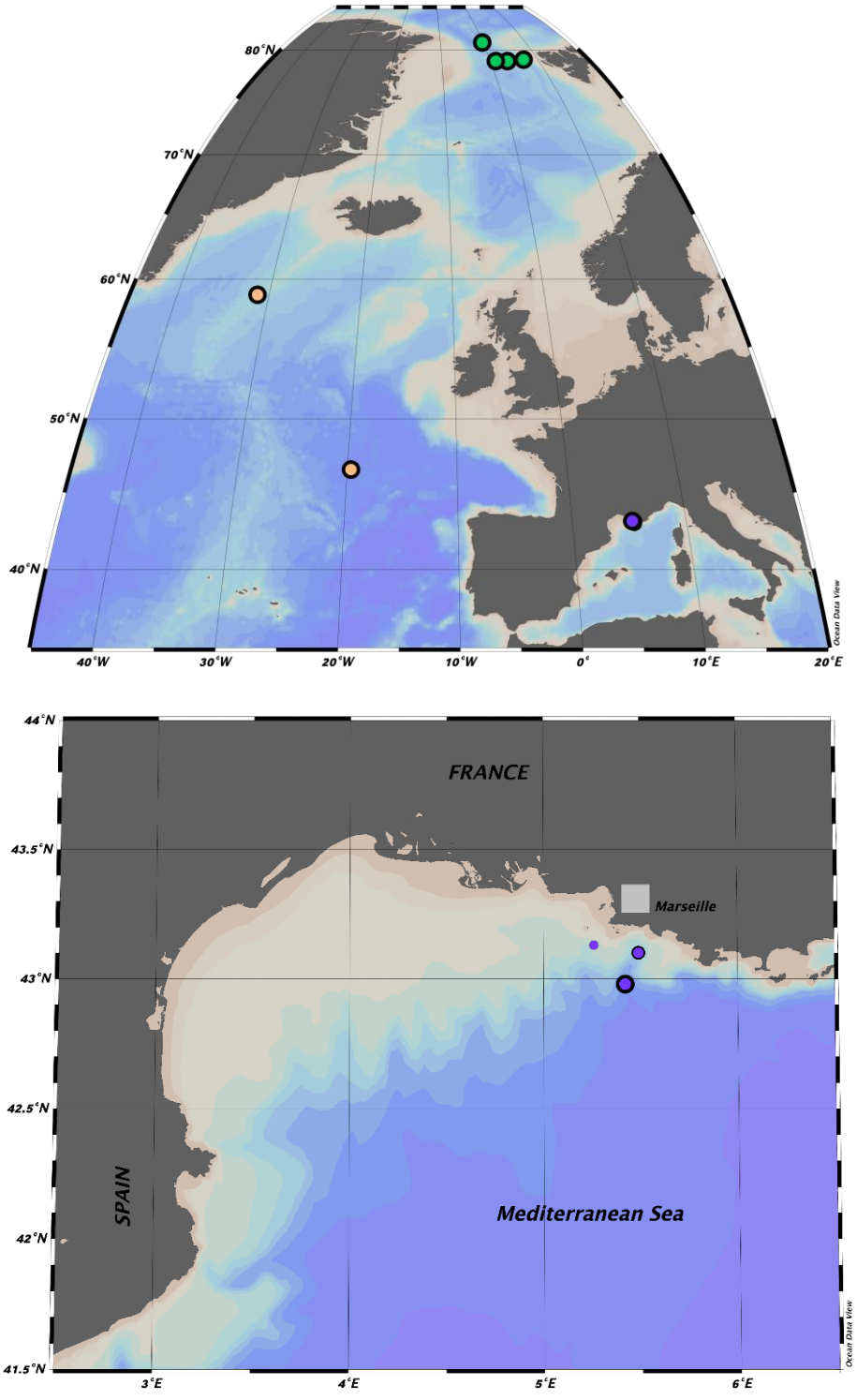

Figure S1. Top: Sampling locations K1, K2 in the Mediterranean Sea (purple), Atlantic Ocean (yellow) and Fram Strait (green). Bottom: Zoom on the 4 Mediterranean locations, with main station K2 (large purple circle), and pHg station K1 and Julio (small purple circles), and Endoume pier in Marseille Bay (grey square).

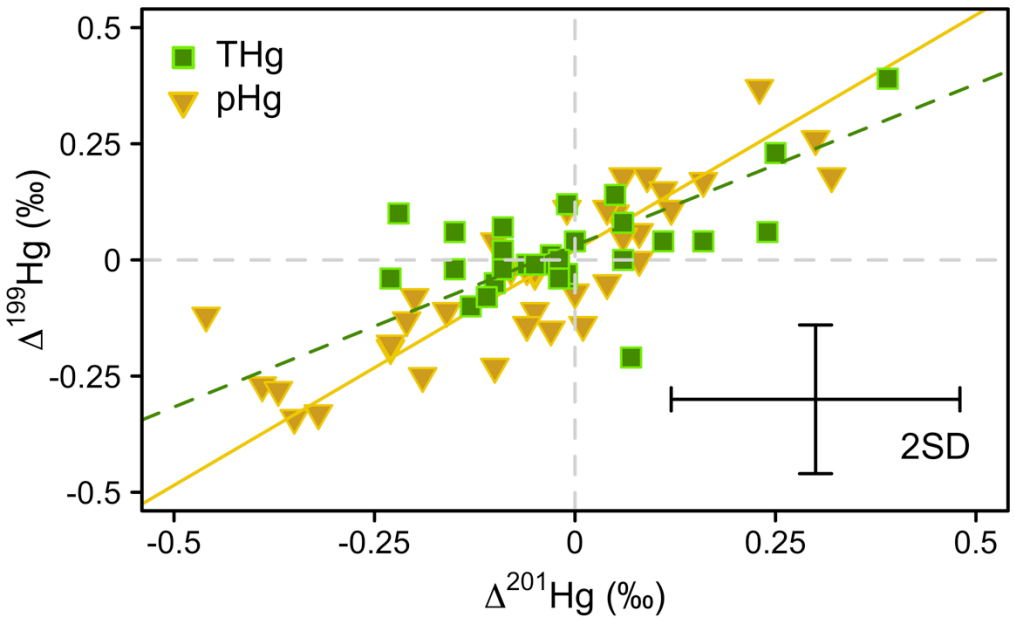

Figure S2: Scatterplot of odd Hg isotope mass-independent fractionation, Δ^{201}Hg vs. Δ^{199}Hg of all tHg and pHg seawater data, including the published data by Motta et al. 2019. The dashed line represents the York regression using IsoplotR[25] for tHg (Δ^{199}Hg = 0.79(±0.29) Δ^{201}Hg + (0.03±0.04), (± se), MSWD = 0.2). The solid line represents the York regression for pHg (Δ^{199}Hg = 1.01(±0.0.09) Δ^{201}Hg + (0.02±0.02), (± se), MSWD = 1.25). Error bars represent the 2 SD of replicate procedural standards for tHg and pHg.

679

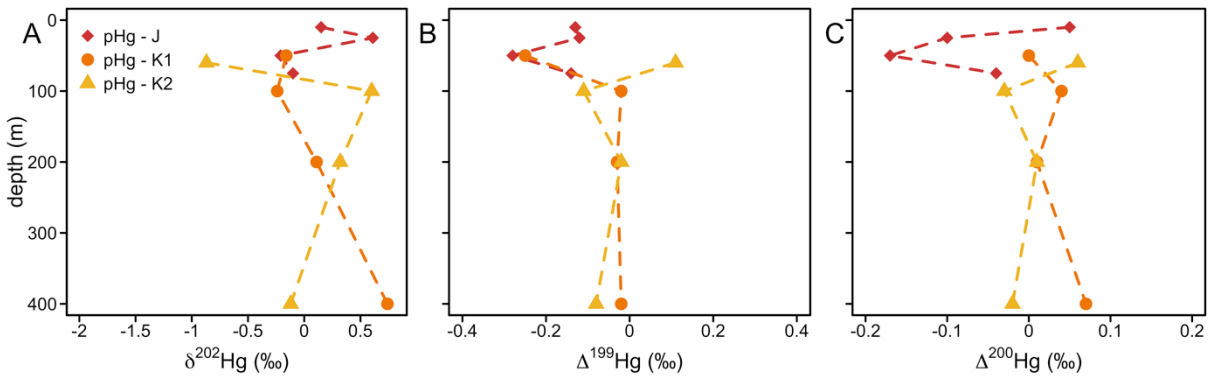

680

681 **Figure S3. Depth profile of particulate Hg stable isotope composition at three stations in the**
682 **Mediterranean during the June 2017 campaign.** A: mass-dependent fractionation (δ^{202}Hg), B: odd
683 mass-independent fractionation (Δ^{199}Hg), C: even mass-independent fractionation (Δ^{200}Hg).

684

685

SI References

1. Gratz, L., Keeler, G., Blum, J. & Sherman, L. S. Isotopic composition and fractionation of mercury in Great Lakes precipitation and ambient air. *Environmental Science and Technology* **44**, 7764–7770 (2010).
2. Sherman, L. S. *et al.* Mass-independent fractionation of mercury isotopes in Arctic snow driven by sunlight. *Nature Geoscience* **3**, 173–177 (2010).
3. Sherman, L. S., Blum, J. D., Keeler, G. J., Demers, J. D. & Dvonch, J. T. Investigation of Local Mercury Deposition from a Coal-Fired Power Plant Using Mercury Isotopes. *Environmental Science & Technology* **46**, 382–390 (2012).
4. Enrico, M. *et al.* Atmospheric mercury transfer to peat bogs dominated by gaseous elemental mercury dry deposition. *Environmental Science & Technology* (2016) doi:10.1021/acs.est.5b06058.
5. Obrist, D. *et al.* Tundra uptake of atmospheric elemental mercury drives Arctic mercury pollution. *Nature* **547**, 201-+ (2017).
6. Chen, J., Hintelmann, H. & Dimock, B. Chromatographic pre-concentration of Hg from dilute aqueous solutions for isotopic measurement by MC-ICP-MS. *Journal of Analytical Atomic Spectrometry* **25**, 1402–1409 (2010).
7. Strok, M., Baya, P. A. & Hintelmann, H. The mercury isotope composition of Arctic coastal seawater. *Comptes Rendus Geoscience* **347**, 368–376 (2015).
8. Jiskra, M., Sonke, J. E., Agnan, Y., Helmig, D. & Obrist, D. Insights from mercury stable isotopes on terrestrial-atmosphere exchange of Hg(0) in the Arctic tundra. *Biogeosciences* **16**, 4051–4064 (2019).
9. Heimbürger, L. E. *et al.* Shallow methylmercury production in the marginal sea ice zone of the central Arctic Ocean. *Scientific Reports* **doi:10.1038/srep10318**, (2015).

10. Demers, J. D., Blum, J. D. & Zak, D. R. Mercury isotopes in a forested ecosystem: Implications for air-surface exchange dynamics and the global mercury cycle. *Global Biogeochemical Cycles* **27**, 222–238 (2013).
11. Motta, L. C. *et al.* Mercury Cycling in the North Pacific Subtropical Gyre as Revealed by Mercury Stable Isotope Ratios. *Global Biogeochemical Cycles* **33**, 777–794 (2019).
12. Sherman, L. S. *et al.* Assessment of mercury exposure among small-scale gold miners using mercury stable isotopes. *Environmental Research* **137**, 226–234 (2015).
13. Wang, Z. *et al.* Mass-dependent and mass-independent fractionation of mercury isotopes in precipitation from Guiyang, SW China. *Comptes Rendus Geoscience* **347**, 358–367 (2015).
14. Donovan, P. M., Blum, J. D., Yee, D., Gehrke, G. E. & Singer, M. B. An isotopic record of mercury in San Francisco Bay sediment. *Chemical Geology* **349**–**350**, 87–98 (2013).
15. Fu, X. W., Marusczak, N., Wang, X., Gheusi, F. & Sonke, J. E. The isotopic composition of total gaseous mercury in the free troposphere of the Pic du Midi Observatory (2877 m a.s.l, France). *Environmental Science & Technology* (2016) doi:10.1021/acs.est.6b00033.
16. Demers, J. D., Sherman, L. S., Blum, J. D., Marsik, F. J. & Dvonch, J. T. Coupling atmospheric mercury isotope ratios and meteorology to identify sources of mercury impacting a coastal urban-industrial region near Pensacola, Florida, USA. *Global Biogeochemical Cycles* **29**, 1689–1705 (2015).
17. Yu, B. *et al.* Isotopic Composition of Atmospheric Mercury in China: New Evidence for Sources and Transformation Processes in Air and in Vegetation. *Environmental Science & Technology* **50**, 9262–9269 (2016).
18. Mil-Homens, M. *et al.* Tracing anthropogenic Hg and Pb input using stable Hg and Pb isotope ratios in sediments of the central Portuguese Margin. *Chemical Geology* **this issue**, (2012).
19. Araujo, B. F. *et al.* Mercury speciation and Hg stable isotope ratios in sediments from Amazon floodplain lakes—Brazil. *Limnology and Oceanography* **63**, 1134–1145 (2018).

20. Senn, D. B. *et al.* Stable Isotope (N, C, Hg) Study of Methylmercury Sources and Trophic Transfer in the Northern Gulf of Mexico. *Environmental Science and Technology* **44**, 1630–1637 (2010).
21. Li, M. *et al.* Assessing Sources of Human Methylmercury Exposure Using Stable Mercury Isotopes. *Environmental Science & Technology* **48**, 8800–8806 (2014).
22. Madigan, D. J. *et al.* Mercury Stable Isotopes Reveal Influence of Foraging Depth on Mercury Concentrations and Growth in Pacific Bluefin Tuna. *Environ. Sci. Technol.* **52**, 6256–6264 (2018).
23. Sackett, D. K. *et al.* Carbon, Nitrogen, and Mercury Isotope Evidence for the Biogeochemical History of Mercury in Hawaiian Marine Bottomfish. *Environ. Sci. Technol.* **51**, 13976–13984 (2017).
24. Blum, J. D., Popp, B. N., Drazen, J. C., Choy, C. N. & Johnson, M. W. Methylmercury production below the mixed layer in the North Pacific Ocean. *Nature Geoscience* **DOI: 10.1038/NGEO1918**, (2013).
25. Vermeesch, P. IsoplotR: A free and open toolbox for geochronology. *Geoscience Frontiers* **9**, 1479–1493 (2018).